Chemical Physics Letters 855 (2024) 141583

Contents lists available at ScienceDirect

Chemical Physics Letters

journal homepage: www.elsevier.com/locate/cplett

Research paper

Breakdown of the molecular orbital picture for X-ray emission of water

Lucas M. Cornetta [a], Vincenzo Carravetta [b,*], Takashi Tokushima [c], Yuka Horikawa [d,e], Jan-Erik Rubensson [f], Joseph Nordgren [f], Hans Ågren [f]

[a] Instituto de Física, Universidade de São Paulo, Rua do Matão 1731, 05508-090 São Paulo, Brazil
[b] IPCF-CNR, via Moruzzi 1, 56124 Pisa, Italy
[c] MAX IV Laboratory, Lund University, Box 118, SE 22100, Lund, Sweden
[d] Graduate School of Sciences and Technology for Innovation, Yamaguchi University, Yamaguchi, Japan
[e] RIKEN SPring-8 center, Sayo, Hyogo, Japan
[f] Division of X-ray Photon Science, Department of Physics and Astronomy, Uppsala University, Box 516, 751 20 Uppsala, Sweden

HIGHLIGHTS

- We establish a first example of K-shell X-ray emission spectra with strong breakdown of the molecular orbital picture: a complete splitting into satellites of the $2a_1$ main peak of water molecule.

GRAPHICAL ABSTRACT

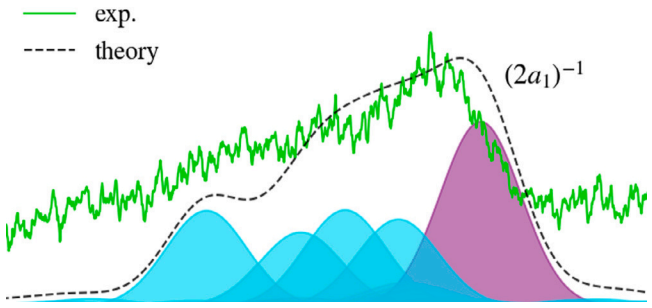

ARTICLE INFO

Keywords:
X-ray emission
Water
MO-breakdown

ABSTRACT

By measuring X-ray emission of the water molecule in liquid phase we establish a first example of K-shell X-ray emission spectra with strong breakdown of the molecular orbital picture. A complete splitting of the $2a_1$ peak into satellites is observed. A theoretical model with electronic configurations generated by coupled excitations/de-excitations, so-called semi-internal configuration interaction, captures the experimentally recorded features well. Differences with respect to the corresponding breakdown effect in ultraviolet photoelectron spectrum are highlighted. Molecular dynamics calculations indicate that solvent broadening can only make up for a small fraction of the width of the recorded $2a_1$ derived band.

1. Introduction

The introduction of high-resolution X-ray emission spectroscopy (XES), almost 50 years ago, made it possible to study X-ray transitions that connect core with valence levels. With this progress one could analyze X-ray spectra in terms of concepts in chemistry, like chemical valence, chemical shifts, molecular orbital theory and electro-vibrational coupling. Over the years a multitude of spectra have been analyzed by molecular orbital (MO) theory, which makes a one-to-one assignment between molecular orbitals and recorded electronic spectral bands; see for instance [1]. A particularly useful feature coupled to MO theory for X-ray emission is the one-center model, introduced several decades ago [2], which has served an operational model both for coarse and quantitative evaluation of X-ray emission spectra, and, reversely, for using X-ray spectra to derive local populations of certain symmetries. It implements the Laporte selection rules for atomic radiative

* Corresponding author.
E-mail address: vincenzo.carravetta@pi.ipcf.cnr.it (V. Carravetta).

https://doi.org/10.1016/j.cplett.2024.141583
Received 26 April 2024; Received in revised form 23 August 2024; Accepted 26 August 2024
Available online 28 August 2024

emission with angular momentum change of one unit in a molecular environment. Applying the molecular orbital picture for X-ray emission offers a theoretical construct of the full spectrum, where the relative energetics is guided by the orbital energies (Koopmans theorem) and the relative intensities by the one-center model.

Outer valence hole states are often well described by MO theory using the independent electron picture, where the leading dynamic electron correlation contributions generally act as small corrections to energy and intensity of the emission bands. The applicability of MO theory and its associated one-center model for XES is though not universal – in electron spectroscopies, like X-ray photoelectron spectroscopy (XPS) and Auger, it is known that inner valence levels might be, or are, less well described by MO theory as these levels are prone to static, near-degenerate, electron correlation effects that split the bands into satellites. A one-to-one assignment of states and MOs is not possible for these satellites, leading to the so-called "breakdown of MO theory". The water molecule has served as a benchmark for the discovery of this effect in photoelectron spectroscopy [3,4] and for Auger [5]. In X-ray emission corresponding effects have been observed for 3s emission in $L_{II,III}$ spectra for solid state (powder) compounds from S to Cr [6], and for Ar [7,8] then termed "semi-Auger" which thus also is a semi-internal configuration interaction effect. Inspecting XES spectra on N_2 [9] and NH_3 [10] one could suspect that splitting, respectively, broadening of the inner valence part could be due to such effects, however, this has not been analyzed. Thus, to the best of our knowledge an analysis of an observation of the breakdown effect has never been provided for XES K-emission giving the breakdown of the molecular orbital picture, for any type of system.

Water has been vigorously studied in XES, both in the gas [11–13] and in the liquid [14–18] phase. The interpretation of the liquid spectra, and its implications for the hydrogen-bond structure and dynamics are still being debated. However, the inner-valence region of the spectra has so far attracted little attention.

That inner valence levels have been less attended in XES, or not observed at all, probably owes to the fact that (for first row molecules) the corresponding MOs are atomic 2s like and therefore XES forbidden by decay of the core hole according to the one-center rule. In this work we take advantage of the capacity of modern synchrotron facilities and make a detailed study on how the breakdown effect may influence XES spectra using the previously benchmark water molecule as example. Some ramifications of the present finding for studies of XES spectra in general are discussed.

2. Measurements

X-ray emission measurements were performed using a slitless emission spectrometer [19] at SPring-8 BL17SU [20]. Pure liquid water purified by a water purifier, Millipore Direct-Q UV, was used as a sample. The sample was flowing through a liquid flow cell that uses an Au-coated 150 nm thick silicon nitride (SiN) membrane (NTT-AT Co. Japan) as a window for soft X-rays. The SiN window was used for separating the flowing liquid under atmospheric pressure from the high vacuum. The incoming probe photons and going-out photons emitted from the sample are transmitted through this window [21]. Excitation energy was tuned to 550 eV and circular polarization was used to avoid unnecessary polarization effects. For evaluation of the natural oxides on the window, acetonitrile, purely >99.5%, Sigma-Aldrich, which does not contain oxygen in the molecular structure, was used. The collected spectra are presented in Fig. 1. The emission signal around 390 eV is coming from N1s emission of the SiN window. For the pure acetonitrile sample, the spectra also contain the contribution of nitrogen in acetonitrile in addition to the SiN window. The peak at 550 eV is the elastic scattering peak. The peaks around 525 eV belong to O 1s emissions of water. The contribution of the natural oxides on the window appears around 525 eV but the intensity is around 10 times weaker than O 1s emission from water. For the energy region from 420 eV to 520 eV, the spectrum is almost flat and the contribution of the natural oxides is negligible. Therefore, the clear peak structure around 505 eV is assignable to the emission from water.

3. Calculations

Theoretical calculations for a single water molecule, at the experimental geometry, were carried out in order to present a characterization of the emission structures associated with the satellite peaks. The investigation was performed at the restricted active space second-order perturbation theory (RASPT2) level of theory, together with the ANO-RCC-VTZP basis set. Relativistic effects were included using the Douglas-Kroll transformation of the relativistic Hamiltonian, together with spin–orbit interactions. The active space comprises the oxygen $1s$ core orbital ($1a_1$) in RAS1 subspace, ($2a_1$)($1b_2$)($3a_1$)($1b_1$) orbitals in RAS2 subspace and ($4a_1$)($5a_1$)($2b_1$)($1a_2$)($2b_2$) orbitals in RAS3 subspace, totalizing 9 electrons in 10 orbitals in which two electrons in RAS3 were allowed. The primary ionized state of the water molecule was described imposing the restriction of one electron in RAS1. Sixteen lowest states for each of the four symmetry components belonging to the C_{2v} point group were considered for the state-averaged convergence of the molecular orbitals and for the configuration interaction procedure. The transition intensities were calculated based on both first (electric dipole) and second order (electric quadrupole and magnetic dipole) transition moments. The calculations were performed with the Molcas package [22].

In order to estimate a possible effect of the condensed phase on the XES spectrum in the considered energy region the spectrum was simulated also for the central molecule in a number of small water clusters (26 water molecules) suggested by short molecular dynamics (MD) calculations. The dynamics of 4166 water molecules in a cubic box of dimension 50 Angstrom, with periodic boundary conditions in x, y and z directions, was simulated using the GROMACS code version 5.1.4 [23,24] and the TIP4P water model [25]. Starting from a random distribution of the molecules, a standard minimization - heating - equilibration protocol was adopted, followed by a production run of 5 ns with a time step of 1 fs. The dynamics for the canonical ensemble (NVT), apart from the heating-equilibration steps, were conducted at $T = 300$ K fixed with a velocity rescaling thermostat. The trajectory was analyzed by sampling the last 2 ns of the simulation in order to identify some representative cluster structures in the liquid phase. The hydrogen bond analysis showed that the clusters with average radius of 6 Angstrom had 5, 4, 3 and 2 hydrogen bonds in a percentage of 5, 41, 35 and 15 respectively. Six clusters were considered: 3 clusters with the first solvation shell formed by 4 waters and 3 clusters with the first solvation shell formed by 3 waters, in order to get insight of the spectrum dependence from the cluster geometry. An explicit core-hole-induced effect on the initial solvent structure has been considered negligible. At most comparable to the structural variability of the environment here investigated by considering six different clusters. We expected that in the case of the $2a_1$ orbital which, being internal, has a small interaction with the solvent, the effect of the environment structure was minor.

In this case the spectrum was computed by DFT calculations with the PD86 density functional [26] and the StoBe version of the deMon code [27]. Such choice allows to include the effect of electron correlation maintaining a single band for the decay from the $2a_1$ Kohn–Sham (KS) MO of the single molecule and then mimic only the effect of the environment in the liquid phase.

4. Discussion

In Fig. 1 the full experimental spectrum of liquid water is shown with its characteristic distribution of outer valence $1b_2$, $3a_1$, $1b_1$ emissions, the latter consisting in a split band. The $2a_1$ derived emission band has, instead, an onset around 490 eV with a slow increasing of the intensity up to 508 eV, followed by a steep decreasing. The presently computed XES spectrum of the water molecule is presented in Fig. 2; Fig. 3 shows a blow up of the region 495–515 eV. The theoretical bands are here assigned an arbitrary broadening factor given by a

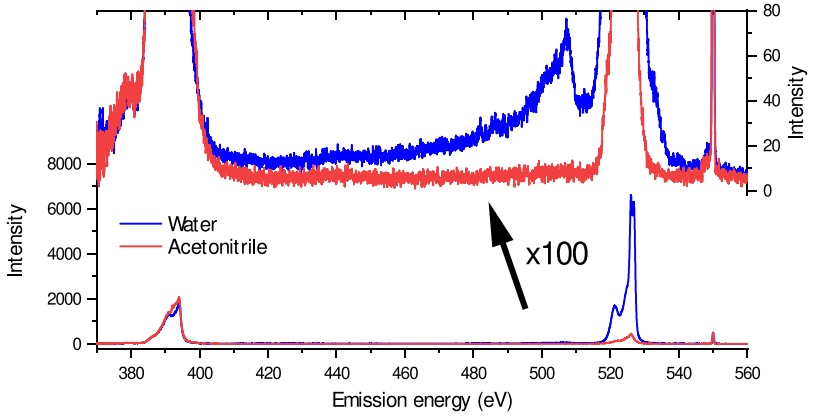

Fig. 1. XES spectra of liquid water (blue lines) and acetonitrile (red lines). The upper panel shows a 100 times magnified version of the spectra in the lower panel.

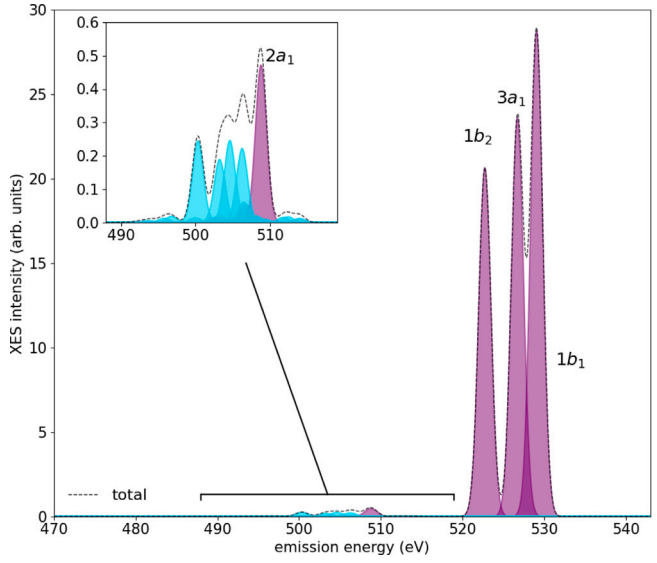

Fig. 2. Computed full XES spectrum of water molecule; upper left panel: magnification of the $2a_1$ energy region.

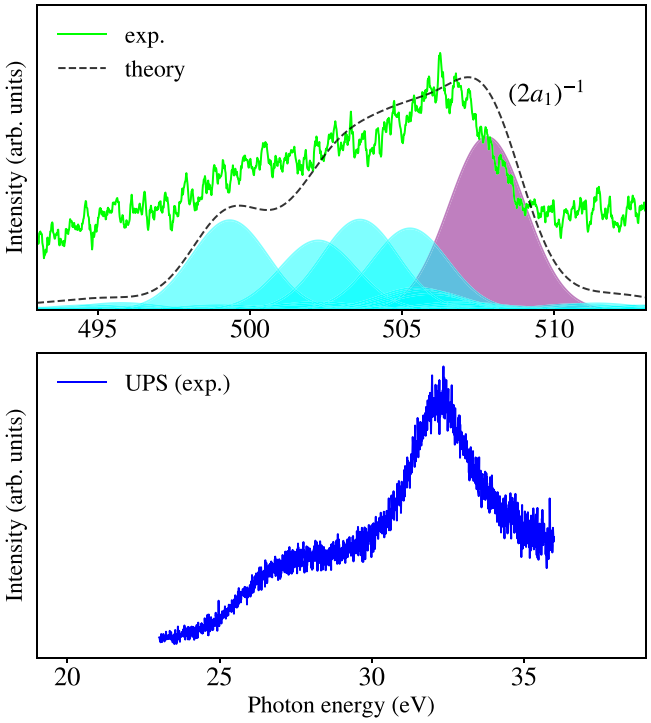

Fig. 3. $2a_1$ inner valence part of XES spectrum of liquid water. Computed transitions, see Table 1, are inserted beneath as Gaussian bands shifted by −1 eV. The threshold photoelectron spectrum (UPS) of water in the $2a_1$ region, measured by Truong et al. [28] is inserted below for comparison.

Gaussian function with FWHM = 3 eV. This is done with the purpose of presenting the theoretical results, obtained in the vertical transition approximation, i.e. for the rigid water molecule at its ground state geometry, in a way that makes it easier a comparison with the poorly resolved experimental band. The broadening is in fact the same for every single theoretical intensity and each gaussian is centered at the computed photon energy. The arbitrary broadening intends to simulate both the effect of the nuclear motion (see below) and that of the average on the local structures of the environment.

Although Fig. 3 shows the computed XES spectrum for a single water molecule, there is a remarkable agreement in the appearance of the $2a_1$ deriving intensity distribution between 495 and 510 eV with the experimental liquid spectrum. Thus the low energy slope of the structure is composed of a number of satellites, the peaky feature at 508 is assigned to the main $2a_1^{-1}$ configuration, while the descending slope towards higher energies is due to a single weak satellite state (see Table 1). Each such state can be assigned through the semi-internal excitation pattern which leads to a mixing of single-hole plus excitation satellite states. For example, the rather strong satellite at 500.34 eV can be explained by a leading $(1b_1)^{-1}(1b_2)^{-1}(1a_2)^1$ configuration. The (atomic) dipole selection rule is overcome by the symmetry breaking for the $2a_1$ orbital and by the presence of satellite states but the integrated intensity of the 490–510 eV features is much smaller than that of the outer valence bands.

Table 1
Main electronic configurations corresponding to the four most intense satellite states in the theoretical spectrum. The intensities are given relatively to the intensity of the strongest $1b_1$ peak at 529.07 eV.

Final state	Symmetry	Emission energy (eV)	Intensity
$(1b_2)^{-1}(1b_1)^{-1}(1a_2)^1$	A_1	500.34	0.0085
$(1b_2)^{-1}(1b_1)^{-1}(2b_2)^1$	B_1	503.24	0.0066
$(1b_2)^{-1}(3a_1)^{-1}(2b_2)^1$	A_1	504.61	0.0086
$(3a_1)^{-1}(1b_1)^{-1}(4a_1)^1$	B_1	506.26	0.0077

The MO breakdown effect has been well-known in ultraviolet photoelectron spectroscopy for a long time, where water has served as a benchmark example, both experimentally e.g. [28,29] and theoretically [30,31]. The threshold photoelectron spectra of water in the $2a_1$ region, measured by Truong et al. is given in Fig. 6 of Ref. [28] and reproduced in the lower panel of Fig. 3. One can there note two main

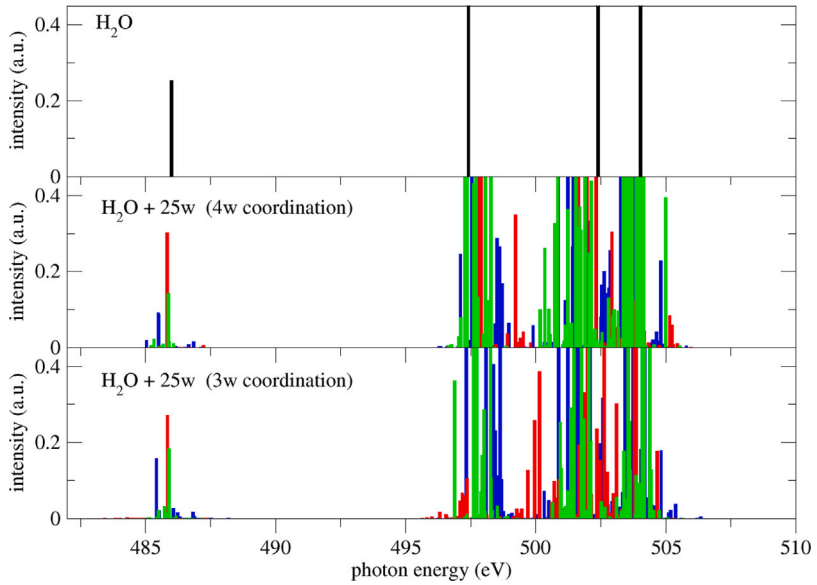

Fig. 4. Theoretical XES spectra of a single water molecule (black bars) and of the central water molecule in different water clusters (blue, red and green bars) computed by DFT (ground state approximation and PD86 functional). Each cluster includes a central water molecule where the core ionization occurs, surrounded by 25 water molecules; the 3 clusters corresponding to the spectra in the middle (bottom) window have 4 (3) waters in the first solvation shell.

very broad bands at 27.6 and 32.3 eV. The latter was assigned to a state with a dominating $2a_1^{-1}$ configuration, the former to a satellite [29,30].

Several weaker satellite states can underlie the broad features; Wood [31] predicted by means of configuration interaction calculations not less than 11 states in the energy region 17.6–29.7 eV. The broadness of the bands can be understood from the work of Tan et al. [32] who used an electron-impact coincidence technique to measure the cross-sections for photo-fragmentation in H_2O, including the $2a_1$ band system. Their spectra showed that H_2O^+ in that region dissociates completely, something that well explains the broad structure-less features of the two bands in the UPS spectrum, and the lack of any sign of vibrational structure in the XES spectrum, in contrast to the outer valence levels. The diminishing slope below 497 eV may receive contributions from higher external excitations, eventually reaching beyond a continuum, in which case the features would correspond to ICD (Intra- or Inter-molecular Coulombic Decay) measured for $2a_1$ holes in water [33].

Subtracting the core ionization potential energy of water from the XES vertical energies one gets “UPS” vertical energies that well reproduce the spectral region of the real UPS spectrum in Fig. 3. As seen the form of the XES and UPS spectra are different, which evidently can be understood by the fact that different initial states and different transition processes are involved. The XES spectrum is predicted with more evenly strong transitions of different symmetry. We note that generally non-resonant X-ray emission spectra contain satellites originating from initial shake-up and shake-off states. As the first shake-up state of water is about 18 eV up from the single core hole state, these initial states cannot be reached by the excitation energy employed for the XES spectrum shown in Fig. 1, which thus is satellite free.

It is well known that the XES spectrum of liquid water is characterized, when compared to that measured in gas phase, by a peculiar splitting, also observable in Fig. 1, of the higher energy narrow band. A question arises, then, about the possible role of the liquid environment also regarding the structures observed in the $2a_1$ region of the XES spectrum. We can expect that the effect of the condensed phase environment on the XES spectrum is limited and cannot explain the large width observed for the $2a_1$ band. In fact, such effect has been invoked, but not definitively proven, for the splitting of the $1b_1$ band which is well below one eV. Furthermore, the influence of the environment, or by a dynamical H-bond effect, on an inner-valence orbital can be expected to be less than that on a lone-pair orbital.

The results obtained by DFT calculations with the StoBe-deMon code [27], the Perdew-86 density functional [26] and the ground state approximation [34], for a single water molecule and the central molecule in six 26-water clusters, are given in Fig. 4. As expected, also in the DFT approximation the decay from the almost spherical inner valence orbital provides a very weak intensity for a single water molecule; about two orders of magnitude lower than that of the valence shell. In the condensed phase (clusters) the “symmetry breakdown” of the $2a_1$ orbital is accentuated by the presence of hydrogen bonds. However an increase in the total intensity in the $2a_1$ region is not predicted, while there is a distribution of the intensity in a range of about 1–2 eV. This is essentially due to the mixing of the $2a_1$ orbital of the central water molecule with a number of molecular orbitals mostly localized on the surrounding water molecules. Such “environmental breakdown” is then predicted to produce a relatively small spreading of the $2a_1$ intensity, confirming that it is the MO breakdown effect explored above that gives rise to the strong intensity spread that is experimentally observed.

5. Conclusion

By a combined experimental and theoretical study of the low energy region, 490 to 510 eV, of the liquid water X-ray emission spectrum, we could establish a breakdown of the MO picture in X-ray emission spectroscopy in that the O 2s derived $2a_1^{-1}$ state is split into a multitude of satellite states, which, to our knowledge, is the first analysis of the kind for K-shell emission of molecules. A computational model based on semi-internal configuration interaction could well capture the measured intensities. A dynamical study using water clusters indicated that the solvent effect gives rise to a distribution that is much narrower than the recorded one, so indirectly supporting the breakdown effect. It is shown that the appearance of the breakdown effect is different compared to the UPS spectrum of water, which has served as the standard spectrum showing this effect in photoelectron spectroscopy. However, in accordance with UPS/XPS it can be argued that the MO breakdown is a common phenomenon for inner valence states and that it readily can lead to new studies of molecular physics and many-body phenomena along with the development of modern synchrotron technology supported by quantum mechanical methods.

CRediT authorship contribution statement

Lucas M. Cornetta: Writing – review & editing, Investigation. **Vincenzo Carravetta:** Writing – review & editing, Investigation, Formal analysis. **Takashi Tokushima:** Writing – review & editing, Investigation. **Yuka Horikawa:** Writing – review & editing, Investigation. **Jan-Erik Rubensson:** Formal analysis, Data curation. **Joseph Nordgren:** Formal analysis. **Hans Ågren:** Writing – original draft, Investigation, Conceptualization.

Declaration of competing interest

The authors declare that they have no known competing financial interests or personal relationships that could have appeared to influence the work reported in this paper.

Data availability

Data will be made available on request.

Acknowledgments

The synchrotron radiation experiments were performed at BL17SU in SPring-8 with the approval of RIKEN (Proposal No. 20150064). We would like to thank Dr. M. Oura for his valuable help with experiments at BL17SU. LMC acknowledges São Paulo Research Foundation (FAPESP) on process nr. 2021/06527-7. HÅ was supported by the Swedish Science Research Council on contract 2022-03405.

References

[1] F. Gel'mukhanov, H. Ågren, Resonant X-ray Raman scattering, Phys. Reps. 312 (1999) 87–330.
[2] R. Manne, J. Chem. Phys. 52 (1970) 5733.
[3] L.S. Cederbaum, Chem. Phys. Lett. 25 (1974) 562.
[4] L.S. Cederbaum, W. Domcke, J. Schirmer, Phys. Scr. 21 (1980) 481.
[5] H. Ågren, H. Siegbahn, Chem. Phys. Lett. 69 (1980) 424.
[6] L Weinhardt, D Hauschild, O Fuchs, R Steininger, N Jiang, M Blum, JD Denlinger, W Yang, E Umbach, C Heske, ACS Omega 8 (2023) 4921.
[7] J.W. Cooper, R.E. LaVilla, Phys. Rev. Lett. 25 (1970) 1975.
[8] J. Nordgren, H. Ågren, C. Nordling, K. Siegbahn, Phys. Scr. 19 (1979) 5.
[9] L.O. Werme, B. Grennberg, J. Nordgren, C. Nordling, K. Siegbahn, Nature 242 (1972) 453.
[10] L. Weinhardt, E. Ertan, M. Iannuzzi, M. Weigand, O. Fuchs, M. Bar, M. Blum, J.D. Denlinger, W. Yang, E. Umbach, M. Odelius, C. Heske, Phys. Chem. Chem. Phys. 17 (2015) 27145.
[11] L.O. Werme, J. Nordgren, H. Ågren, C. Nordling, K. Siegbahn, Z. Phys. A 272 (1975) 131.
[12] Lothar Weinhardt, Andreas Benkert, Frank Meyer, Monika Blum, Regan G. Wilks, Wanli Yang, Marcus Bär, Friedrich Reinert, Clemens Heske, J. Chem. Phys. 136 (14) (2012) 144311, http://dx.doi.org/10.1063/1.3702644, arXiv:https://pubs.aip.org/aip/jcp/article-pdf/doi/10.1063/1.3702644/15450703/144311_1_online.pdf.
[13] Vinícius Vaz da Cruz, Faris Gel'mukhanov, Sebastian Eckert, Marcella Iannuzzi, Emelie Ertan, Annette Pietzsch, Rafael C Couto, Johannes Niskanen, Mattis Fondell, Marcus Dantz, Thorsten Schmitt, Xingye Lu, Daniel McNally, Raphael M Jay, Victor Kimberg, Alexander Föhlisch, Michael Odelius, Nature Commun. 10 (2019) 1013, http://dx.doi.org/10.1038/s41467-019-08979-4.
[14] J H Guo, Y Luo, A Augustsson, J E Rubensson, C Såthe, H Ågren, H Siegbahn, J Nordgren, Phys. Rev. Lett. 89 (2002) 137402.
[15] O. Fuchs, M. Zharnikov, L. Weinhardt, M. Blum, M. Weigand, Y. Zubavichus, M. Bär, F. Maier, J.D. Denlinger, C. Heske, M. Grunze, E. Umbach, Phys. Rev. Lett. 100 (2008) 027801, http://dx.doi.org/10.1103/PhysRevLett.100.027801, URL https://link.aps.org/doi/10.1103/PhysRevLett.100.027801.
[16] Thomas Fransson, Yoshihisa Harada, Nobuhiro Kosugi, Nicholas A Besley, Bernd Winter, John J Rehr, Lars GM Pettersson, Anders Nilsson, Chem. Rev. 116 (2016) 7551–7569, http://dx.doi.org/10.1021/acs.chemrev.5b00672.
[17] Johannes Niskanen, Mattis Fondell, Christoph J. Sahle, Sebastian Eckert, Raphael M. Jay, Keith Gilmore, Annette Pietzsch, Marcus Dantz, Xingye Lu, Daniel E. McNally, Thorsten Schmitt, Vinicius Vaz da Cruz, Victor Kimberg, Faris Gel'mukhanov, Alexander Föhlisch, Proc. Natl. Acad. Sci. 116 (2019) 4058–4063, http://dx.doi.org/10.1073/PNAS.1815701116, URL https://www.pnas.org/content/116/10/4058.
[18] Harada, et al., J. Phys. Chem. Lett. (2017) 5487–5491.
[19] T. Tokushima, Y. Horikawa, S. Shin, Rev. Sci. Instrum. 82 (7) (2011) 073108, http://dx.doi.org/10.1063/1.3610454, arXiv:https://pubs.aip.org/aip/rsi/article-pdf/doi/10.1063/1.3610454/16007842/073108_1_online.pdf.
[20] Haruhiko Ohashi, Yasunori Senba, Hikaru Kishimoto, Takanori Miura, Eiji Ishiguro, Tomoyuki Takeuchi, Masaki Oura, Katsutoshi Shirasawa, Takashi Tanaka, Masao Takeuchi, Kunikazu Takeshita, Shunji Goto, Sunao Takahashi, Hideki Aoyagi, Mutsumi Sano, Yukito Furukawa, Toru Ohata, Tomohiro Matsushita, Yasuhide Ishizawa, Shingo Taniguchi, Yoshihiro Asano, Yoshihisa Harada, Takashi Tokushima, Koji Horiba, Hideo Kitamura, Tetsuya Ishikawa, Shik Shin, AIP Conf. Proc. 879 (1) (2007) 523–526, http://dx.doi.org/10.1063/1.2436113, arXiv:https://pubs.aip.org/aip/acp/article-pdf/879/1/523/12065067/523_1_online.pdf.
[21] Takashi Tokushima, Yuka Horikawa, Yoshihisa Harada, Osamu Takahashi, Atsunari Hiraya, Shik Shin, Phys. Chem. Chem. Phys. 11 (2009) 1679–1682, http://dx.doi.org/10.1039/B818812B.
[22] Ignacio Fdez. Galván, Morgane Vacher, Ali Alavi, Celestino Angeli, Francesco Aquilante, Jochen Autschbach, Jie J. Bao, Sergey I. Bokarev, Nikolay A. Bogdanov, Rebecca K Carlson, et al., J. Chem. Theory Comput. 15 (2019) 5925, http://dx.doi.org/10.1021/acs.jctc.9b00532, arXiv:https://doi.org/10.1021/acs.jctc.9b00532. PMID: 31509407.
[23] M.J. Abraham, et al., SoftwareX (2015) 19–25.
[24] D. Van Der Spoel, et al., J. Comput. Chem. (2005) 1701–1718.
[25] W.L. Jorgensen, J. Chandrasekhar, J.D. Madura, R.W. Impey, M.L. Klein, J. Chem. Phys. (1983) 926–935, http://dx.doi.org/10.1063/1.445869.
[26] J.P. Perdew, Y. Wang, Phys. Rev. B 33 (1986) 8800.
[27] K. Hermann, L.G.M. Pettersson, M.E. Casida, C. Daul, A. Goursot, A. Koester, E. Proynov, A. St-Amant, D.R. Salahub, Contributing authors: V. Carravetta, H. Duarte, C. Friedrich, N. Godbout, M. Gruber, J. Guan, C. Jamorski, M. Leboeuf, M. Leetmaa, M. Nyberg, S. Patchkovskii, L. Pedocchi, F. Sim, L. Triguero, A. Vela, StoBe-deMon version 3.3, 2014.
[28] S.Y. Truong, A.J. Yencha, A.M. Juarez, Cavanagh, P. Bolognesi, G.C. King, Chem. Phys. 355, 183.
[29] N. Martensson, P.A. Malmquist, S. Svensson, E. Basilier, J.J. Pireaux, U. Gelius, K. Siegbahn, Nouveau J. Chim. 1 (1977) 191.
[30] L.S. Cederbaum, Ph.D. thesis, University of Munich, 1971.
[31] M. Wood, Chem. Phys. 5 (1974) 471.
[32] K.H. Tan, C.E. Brion, Ph.E. Van Der Leeuw, M.J. Van Der Wiel, Chem. Phys. 29 (1978) 299.
[33] P. Zhang, C. Perry, T. Trung Luu, D. Matselyukh, H.J. Wörner, Phys. Rev. Lett. 128 (2022) 133001.
[34] L. Triguero, et al., J. Phys. Chem. A (1998) 10599.